EFFICIENT SAMPLING OF SPARSE WIDEBAND ANALOG SIGNALS

Moshe Mishali and Yonina C. Eldar

Department of Electrical Engineering
Technion - Israel Institute of Technology
Haifa, Israel 32000
{moshiko@tx,yonina@ee}.technion.ac.il

Joel A. Tropp

Applied & Computational Mathematics
California Institute of Technology
Pasadena, CA 91125-5000
jtropp@acm.caltech.edu

ABSTRACT

Periodic non-uniform sampling is a known method to sample signals whose spectrum is sparsely occupied at rates below Nyquist. However, this strategy relies on the implicit assumption that the individual samplers are exposed to the entire frequency range. This assumption becomes impractical for wideband sparse signals. In this paper, we propose an alternative sampling stage that does not require a full-band front end. Instead, we suggest an analog front-end that consists of a bank of multipliers, and low-pass filters with cut-off much lower than the Nyquist rate. We then show that the problem of recovering the reginal signal from the low-rate samples can be studied within the framework of analog compressed sensing. We derive a parameter selection under which this system uniquely determines the analog input and address stability aspects of the corresponding reconstruction. Numerical experiments demonstrate robust recovery in the presence of additive noise.

Index Terms— Analog to digital conversion, compressed sensing, infinite measurement vectors (IMV), multi band sampling.

1. INTRODUCTION

Radio-frequency (RF) technology allows to modulate narrow bandwidth transmissions over relatively high carrier frequencies. A wideband RF signal is said to be sparse if it contains only several such transmissions so that the total transmission bandwidth occupies a small portion of the spectrum. Sampling a wideband signal at the Nyquist rate has long become prohibitive as carrier frequencies pass the rates of state-of-the-art analog to digital converters (ADCs) by orders of magnitude. Thus, exploiting the inherent sparsity is necessary to reduce conversion-rate. A multi band signal is a convenient model which captures the sparsity structure by restricting the frequency support to reside within several continuous intervals (bands) and vanish elsewhere.

Previous work on multi band signals reduced the sampling rate by taking point-wise samples of the analog signal on a periodic non-uniform grid [1]. Multi coset sampling, a specific strategy of this type, was analyzed in [2] and proved to allow exact recovery when band locations are known. Blind recovery, namely recovery in the case band locations are unknown, was studied extensively in [3]. However, the sampling front ends of [1–3] are impractical for wideband applications, since standard ADCs require matching their specified rate to the Nyquist rate of the input signal even when the actual sampling rate is lower. Other limitations are detailed in Section 2.2. A recent work considered a hybrid optic-electronic sampling scheme which can partially overcome these limitations [4], at the expense of size and cost.

In this paper, we propose a practical sampling system consisting of two stages: a front-end (non-optical) hardware and standard low-rate ADCs. Our system design is inspired by the one-channel random demodulator of [5], which was used for a discrete signal model. In contrast, our method assumes an analog input signal, no randomness, and the digital conversion is carried out in several parallel channels. After reviewing some necessary background material, in Section 2, we describe the proposed design in Section 3. Frequency domain analysis then leads to an infinite measurement vectors system, which allows to infer the band support from a finite dimensional program [6]. The latter can be solved within the framework of compressed sensing (CS). We prove that a certain parameter selection guarantees a unique analog signal matching the samples. Additional requirements for stable recovery are also detailed. Numerical experiments, provided in Section 4, are used to evaluate the design and to demonstrate stable recovery in the presence of noise.

This work was supported in part by the Israel Science Foundation under Grant no. 1081/07 and by the European Commission in the framework of the FP7 Network of Excellence in Wireless COMmunications NEWCOM++ (contract no. 216715).

2. FORMULATION AND BACKGROUND

2.1. Design Goals for Efficient Sampling

Let $x(t)$ be a real-valued finite-energy signal in the time domain, and $X(f) = \int_{-\infty}^{\infty} x(t) \exp(-j2\pi f t) dt$ be its Fourier transform (assumed to exist). In the sequel, we consider a multi band signal model $\mathcal{M}$ such that every $x(t) \in \mathcal{M}$ is bandlimited to $\mathcal{F} = [-f_{\mathrm{NYQ}}/2, f_{\mathrm{NYQ}}/2]$ and the support of $X(f)$ consists of $2N$ frequency intervals, at the most, of widths not greater than B. Fig. 1 depicts a typical communication application that obeys this signal model.

We wish to design a sampling system for $x(t) \in \mathcal{M}$ under the following requirements:

1. Sampling rate should be as low as possible;
2. Blindness, namely no prior knowledge on band locations;
3. Practical implementation with existing devices.

A sampling stage satisfying these requirements is referred to herein as *efficient*.

The set $\mathcal{M}$ is a union of subspaces corresponding to all possible signal supports. Every $x(t) \in \mathcal{M}$ lies in one of these subspaces. Blindness, is a factor of efficient sampling, since detecting the exact subspace, prior to sampling, may be impossible or too expensive to implement.

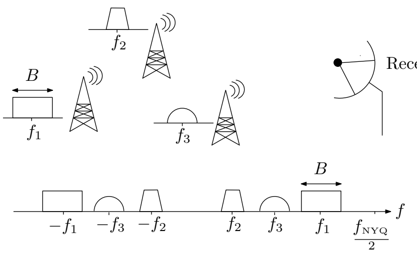

Fig. 1: Three RF transmissions are carried over different carriers f_i. At the receiver, the transmissions sum up to a multi band signal (bottom drawing). In this example $N = 3$, and the modulation techniques of the transmitters determine the maximal expected width B.

The lowest (average) sampling rate which allows blind perfect reconstruction for all signals in $\mathcal{M}$ is $4NB$ samples/sec [3]. This rate is proportional to the effective bandwidth of $x(t)$ and is typically far less than the Nyquist rate f_{NYQ}, which accounts for the maximal possible frequency in $x(t)$. In practice, a sampling rate above $4NB$ is required to allow stable recovery, as further discussed in Section 3.3.

Our previous work describes blind reconstruction of $x(t) \in \mathcal{M}$ from multi coset samples taken at the minimal rate [3]. The next section details the practical limitations of multi coset strategy, which make it inefficient for wideband signals.

2.2. Practical Limitations of Multi Coset Sampling

Multi coset is a periodic non-uniform sampling of the Nyquist rate sequence $x(nT_{\text{NYQ}})$, where $T_{\text{NYQ}} = 1/f_{\text{NYQ}}$. The ith coset takes the ith value in every block of L consecutive samples. Retaining only $p < L$ cosets, indexed by $C = \{c_i\}_{i=1}^{p}$, gives p sequences

$$x_{c_i}[n] = \begin{cases} x(nT_{\text{NYQ}}) & n = mL + c_i, m \in \mathbb{Z} \\ 0 & \text{otherwise}, \end{cases} \tag{1}$$

with an average sampling rate $p/(LT_{\text{NYQ}})$, which is lower than the Nyquist rate.

To explain the practical limitations of this strategy, observe that standard ADC device have a specified maximal rate r, and manufactures require a preceding low-pass filter with cutoff $r/2$. Distortions occur if the anti-aliasing filter is not used, since the design is tailored to $r/2$-bandlimited signals and has an internal parasitic response to frequencies above $r/2$. To avoid these distortions, an ADC with r matching the Nyquist rate of the input signal must be used, even if the actual sampling rate is below the maximal conversion rate r. In multi coset each sequence $x_{c_i}[n]$ corresponds to uniform sampling at rate $1/(LT_{\text{NYQ}})$ whereas the input $x(t)$ contains frequencies till $f_{\text{NYQ}}/2$. Acquiring $x_{c_i}[n]$ is thus possible only if using an ADC with $r = f_{\text{NYQ}}$, which is operated L times slower than its maximal rate. Besides the resource waste, this renders multi coset impractical in wideband applications, in which f_{NYQ} is higher (typically by orders of magnitude) than the rate r of available devices.

A recent work pursued a non-conventional ADC design for wideband applications, which incorporates high-rate optical devices [4]. The hybrid optic-electronic system allows sampling at rate $1/(LT_{\text{NYQ}})$ with minimal attenuation to higher frequencies (till $f_{\text{NYQ}}/2$). Unfortunately, to-date such a result cannot be accomplished purely by electronic technology. Thus, for a variety of wideband applications, which cannot afford the size or expense of an optical system, multi coset sampling becomes impractical.

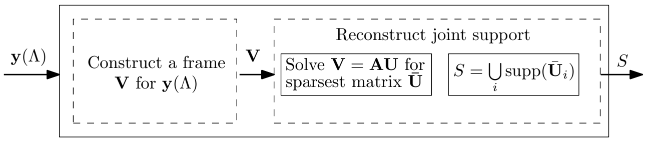

Fig. 2: Recovery of the joint support $S = \text{supp}(\mathbf{x}(\Lambda))$.

Another limitation of multi coset sampling, which also exists in the optical implementation, is maintaining accurate time delays between the ADCs of different cosets. Any uncertainty in these delays impacts the recovery from the sampled sequences.

Before describing the way our proposed sampling stage overcomes these limitations, we briefly review the mechanism underlying the blind reconstruction of [3].

2.3. IMV System

Let $\mathbf{A}$ be a given $m \times n$ matrix with $m < n$ and consider the parametric linear system:

$$\mathbf{y}(\lambda) = \mathbf{A}\mathbf{x}(\lambda), \quad \lambda \in \Lambda, \tag{2}$$

where Λ is some known set (of finite or infinite cardinality). In (2), the unknowns are the vectors $\mathbf{x}(\lambda)$, which are assumed to be jointly K-sparse in the following sense. Define the vector support $\text{supp}(\mathbf{v}) = \{i \,|\, \mathbf{v}_i \neq 0\}$, and the support of the vector set $\mathbf{x}(\Lambda) = \{\mathbf{x}(\lambda) \,|\, \lambda \in \Lambda\}$ as $\text{supp}(\mathbf{x}(\Lambda)) = \cup_\lambda \text{supp}(\mathbf{x}(\lambda))$. Then, $\mathbf{x}(\Lambda)$ is jointly K-sparse if the set size $|\text{supp}(\mathbf{x}(\Lambda))| \leq K$. Put differently, $\mathbf{x}(\Lambda)$ share a common non-zero location set of cardinality K.

When the support $S = \text{supp}(\mathbf{x}(\Lambda))$ is known, recovering $\mathbf{x}(\Lambda)$ from the known vector set $\mathbf{y}(\Lambda) = \{\mathbf{y}(\lambda) \,|\, \lambda \in \Lambda\}$ is possible if the sub-matrix $\mathbf{A}_S$, consisting of the columns of $\mathbf{A}$ indicated by S, has full column rank. In this case,

$$\mathbf{x}_S(\lambda) = (\mathbf{A}_S)^\dagger \mathbf{y}(\lambda) \tag{3a}$$

$$\mathbf{x}_i(\lambda) = 0, \quad i \notin S \tag{3b}$$

where $\mathbf{x}_S(\lambda)$ contains only the entries of $\mathbf{x}$ which are indicated by S, $\mathbf{A}_S^H$ denotes the conjugate transpose of $\mathbf{A}_S$ and $(\mathbf{A}_S)^\dagger = (\mathbf{A}_S^H \mathbf{A}_S)^{-1} \mathbf{A}_S^H$ is the Moore-Penrose pseudo-inverse. For unknown support S, (2) is still invertible if $K = |S|$ is known, and every $2K$ columns of $\mathbf{A}$ are linearly independent [6, 7]. However, solving (2) for $\mathbf{x}(\Lambda)$ is now NP-hard, since recovering S requires a combinatorial search in general. Nonetheless, recent advances in the CS literature provide sub-optimal polynomial-time recovery algorithms for $\mathbf{x}(\Lambda)$, when Λ is a single or a finite element set, corresponding to a single/multiple measurement vectors (SMV/MMV) system [7–12].

Recovering $x(t)$ from multi coset samples boils down to recovering a jointly K-sparse solution of a certain infinite measurement vectors (IMV) system, namely (2) with infinite cardinality Λ. The infinite dimensions are a direct consequence of the relation to a continuous signal $x(t)$. Known band locations imply the support set S, and thus reconstruction is carried out by (3) [1, 2] . In a blind scenario, it was proved in [3, 6] that $\mathbf{x}(\Lambda)$ can be recovered exactly in two steps. First, construct a frame $\mathbf{V}$ for $\mathbf{y}(\Lambda)$ with finitely many vectors. Computing $\mathbf{V}$ translates to simple operations on the sampled sequences, as described in Section 4.2. Then, solve the MMV system $\mathbf{V} = \mathbf{A}\mathbf{U}$ for the matrix $\bar{\mathbf{U}}$ with the minimal number of rows that are non-identically zero. The MMV is guaranteed to have a unique sparse solution $\bar{\mathbf{U}}$ and $S = \cup_i \text{supp}(\bar{\mathbf{U}}_i)$ when the union is

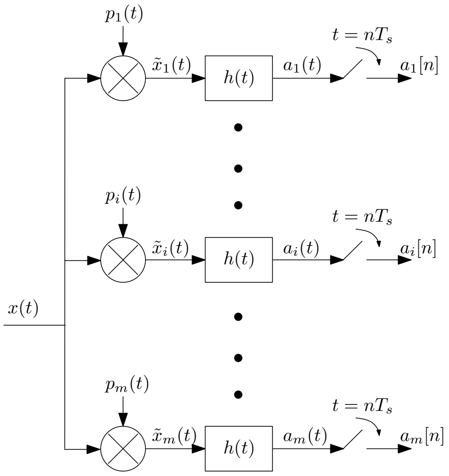

Parameters:

Symbol	Meaning
m	number of sampling channels
T_p	period of each $p_i(t)$
M	number of ± 1 intervals in each period of $p_i(t)$
α_{ik}	the value $p_i(t)$ takes on the kth interval
T_s	time-interval between ADC samples, corresponding to cutting frequency of $h(t)$

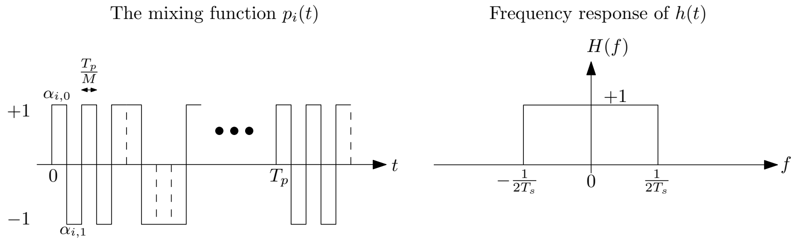

Fig. 3: Description of a practical sampling stage for multi band signals.

taken over the columns of $\bar{\mathbf{U}}$ [6]. Fig. 2 summarizes these recovery steps.

In the next section, we describe and analyze our candidate sampling system. In contrast to multi coset strategy, our system uses low-rate standard ADCs. We match the analog input of the ADCs to their maximal rate. Time offsets between devices are also avoided in the proposed system. Furthermore, the sampling sequences in our method are related to $x(t)$ via an IMV system, although they are different from (1). Consequently, the recovery of $x(t)$ can be performed by using the steps described in Fig. 2 and (3).

3. EFFICIENT SAMPLING

3.1. Description

We now describe the system, as appears in the drawings of Fig. 3. The exact choice of system parameters is described in the next sections.

The signal $x(t)$ enters m channels simultaneously. At the ith channel, $x(t)$ is multiplied by a function $p_i(t)$, referred to as *a mixing function*, and then low-pass filtered and sampled. Each $p_i(t)$ is a T_p-periodic piecewise constant function, which alternates between ± 1 for M equal-length time intervals. Formally,

$$p_i(t) = \alpha_{ik}, \quad k\frac{T_p}{M} \leq t \leq (k+1)\frac{T_p}{M}, \quad 0 \leq k \leq M-1, \quad (4)$$

with $\alpha_{ik} \in \{+1, -1\}$, and $p_i(t + nT_p) = p_i(t)$ for every $n \in \mathbb{Z}$.

Once multiplied by the ith mixing function, actual conversion to digital is carried out by a low-pass filter with a cutoff frequency $1/(2T_s)$ and sampling at rate $1/T_s$. The average sampling rate is therefore m/T_s. Observe the match between the filter cutoff frequency and the ADC sampling rate, and in addition the simultaneous sampling at all channels, which allows for practical implementation. Another advantage of our system is that the new samples are produced at a constant rate, which allows passing them directly to a digital signal processor operating at the same frequency. In contrast, multi coset samples are generated non-uniformly in time, requiring additional hardware to buffer them into digital devices.

3.2. Analysis

To ease exposition we choose an odd M, $T = M/f_{\text{NYQ}}$, and $T_s = T_p = T$. These choices are relaxed in [13]. Consider the ith channel. Since $p_i(t)$ is periodic, it has a Fourier expansion

$$p_i(t) = \sum_{n=-\infty}^{\infty} c_{in} e^{j\frac{2\pi}{T}nt}, \quad (5)$$

where the coefficients are given by [13]

$$c_{in} = \frac{1}{2\pi}\left(\sum_{k=0}^{M-1} \alpha_{ik} e^{-j\omega_0 nk}\right) \frac{1 - e^{-j\omega_0 n}}{jn}, \quad (6)$$

for $\omega_0 = 2\pi/M$ and $c_{in} = c_{i,-n}$. Expressing the Fourier transform $P_i(f)$ in terms of the Fourier series coefficients c_{in} leads to

$$P_i(f) = \int_{-\infty}^{\infty} p_i(t) e^{-j2\pi ft} dt = \sum_{n=-\infty}^{\infty} c_{in}\delta\left(f - \frac{n}{T}\right), \quad (7)$$

with $\delta(t)$ denoting the Dirac delta function. The analog multiplication $\tilde{x}_i(t) = x(t)p_i(t)$ translates to convolution in the frequency domain,

$$\tilde{X}_i(f) = X(f) * P_i(f) = \sum_{n=-\infty}^{\infty} c_{in} X\left(f - \frac{n}{T}\right). \quad (8)$$

Therefore, $\tilde{X}_i(f)$ is a linear combination of shifted copies of $X(f)$.

Filtering $\tilde{X}_i(f)$ by $H(f)$, whose frequency response is an ideal rect function in the interval $\mathcal{F}_0 = [-1/(2T), 1/(2T)]$, results in

$$A_i(f) = H(f)\tilde{X}_i(f) = \sum_{n=-n_0}^{n_0} c_{in} X\left(f - \frac{n}{T}\right), \quad f \in \mathcal{F}_0, \quad (9)$$

where n_0 is the smallest integer satisfying

$$2n_0 + 1 \geq T f_{\text{NYQ}}. \quad (10)$$

Under the choices above, $n_0 = (M-1)/2$. The discrete-time Fourier transform of $a_i[n]$ is

$$A_i(e^{j2\pi fT}) = \sum_{n=-\infty}^{\infty} a_i[n]e^{-j2\pi fTn} \tag{11}$$

$$= \sum_{n=-n_0}^{n_0} c_{in}X\left(f - \frac{n}{T}\right), \quad f \in \mathcal{F}_0. \tag{12}$$

Substituting (6) in (12) leads to the system

$$\mathbf{y}(f) = (\mathbf{SF})(\mathbf{Dx}(f)), \quad f \in \mathcal{F}_0, \tag{13}$$

where $\mathbf{y}_i(f) = A_i(e^{j2\pi fT})$, $1 \le i \le m$, $\mathbf{S}$ is an $m \times M$ matrix whose ikth entry $\mathbf{S}_{ik} = \alpha_{ik}$. The $M \times M$ matrix $\mathbf{F}$ is a certain cyclic columns shift of the discrete Fourier transform matrix of order M. The M-square diagonal $\mathbf{D}$ scales $\mathbf{x}_i(f) = X(f + (i - n_0 - 1)/T)$ according to the last term in (6). Since $\mathbf{D}$ has non-zero diagonal entries, it can be absorbed into $\mathbf{x}(f)$ while keeping $\text{supp}(\mathbf{x}(\mathcal{F}_0)) = \text{supp}(\mathbf{Dx}(\mathcal{F}_0))$. Thus, (13) is an IMV system with $\mathbf{SF}$ replacing $\mathbf{A}$ of (2).

3.3. Parameter Selection and Stable Recovery

The following theorem, whose proof appears in [13], suggests a parameter selection for which the sequences $a_i[n], 1 \le i \le m$ match a unique $x(t) \in \mathcal{M}$. The same selection with only half of the sampling channels can be used for known band locations. Evidently, the system of Fig. 3 can also replace the multi coset stage of [2].

Theorem 1 (Uniqueness) *Let $x(t) \in \mathcal{M}$ be a multi band signal and assume the choices $T = M/f_{\text{NYQ}}$ for an integer M (not necessarily odd) and $T_p = T_s = T$. If:*

1. *$M \le f_{\text{NYQ}}/B$,*
2. *$m \ge 2N$ for non-blind reconstruction or $m \ge 4N$ for blind,*
3. *$\mathbf{S} = \{\alpha_{ik}\}$ is such that every $4N$ columns are linearly independent,*

then, for every $f \in \mathcal{F}_0$, the vector $\mathbf{x}(f)$ is the unique $2N$-sparse solution of (13).

The parameter selection of Theorem 1 guarantees an average sampling rate $m/T \ge 4NB$. Depending on whether f_{NYQ}/B is an integer, this selection allows to achieve the minimal rate when taking the extreme values for m, M. Note that $\mathbf{x}(f)$ is $2N$-sparse, while $\mathbf{x}(\mathcal{F}_0)$ is jointly $4N$-sparse under the parameter selection of the theorem. As detailed in [3], this factor requires doubling m in order to use Fig. 2 and (3). Gaining back this factor at the expense of a higher recovery complexity is also described in [3].

Selecting a specific sign pattern α_{ik} which satisfy the requirement of the theorem is difficult, since validating the condition requires checking the rank of every column subset of $\mathbf{S}$ of cardinality $4N$. Fortunately, the CS literature provides a nice way to overcome this limitation; drawing $\alpha_{ik} = \pm 1$ independently with equal probability is most likely to satisfy the condition of Theorem 1 [8]. In fact, an even stronger condition, termed the restricted isometry property (RIP), holds in this setting [8].

To be precise, recall that a matrix $\mathbf{A}$ is said to have the RIP of order K, if there exists $0 \le \delta_K < 1$ such that

$$(1 - \delta_K) \le \|\mathbf{Ax}\|^2 \le (1 + \delta_K), \tag{14}$$

for every K-sparse unit-norm $\mathbf{x}$ [8]. If $\mathbf{A} = \mathbf{SF}$ satisfies the RIP of order $4N$, then the left hand side of (14) ensures that every $4N$ columns of $\mathbf{A}$ are linearly independent. Since $\mathbf{F}$ is unitary, it implies the condition of the theorem for α_{ik}. Moreover, under the parameter selection of the theorem, every $\mathbf{x}(f)$ in (13) is $2N$-sparse. Thus, the RIP of order $4N$ also ensures that both $\mathbf{A}_S, (\mathbf{A}_S)^\dagger$ are well conditioned for every possible $|S| \le 4N$. This implies stable recovery, in the sense of bounded reconstruction error for bounded errors in the samples [13].

In order to quantify the conditions on m, M under which the RIP of order $4N$ holds, we quote with the following CS results for random matrices. The RIP of order K holds with high probability for a random $m \times M$ matrix $\mathbf{SF}$, for $\mathbf{S}$ with equal probability entries $\mathbf{S}_{ik} = \pm 1/\sqrt{m}$, and a deterministic unitary matrix (such as $\mathbf{F}$ in (13)), if $m \ge C \log(M/K)K$ for some $C > 0$ independent of m, M, K [14]. The necessity of such a log factor, for an alternative RIP definition, was proved in [15]. However, the matrix $\mathbf{S} = \{\alpha_{ik}\}$ in our system is not random and is chosen only once. Nonetheless, baring in mind these results for random matrices, implies a rough relation of $m \ge C \log(M/N)N$ for stable recovery. In practice, we follow the line of many CS papers, and suggest to evaluate the stability of a specific chosen $S = \{\alpha_{ik}\}$ implicitly in simulations, as performed in the next section.

4. NUMERICAL EVALUATION

To complete the design criteria for our system, we conduct two experiments. First, the influence of different sign patterns α_{ik} on the recovery is examined. Then, recovery in the presence of input noise, $x(t) + n(t)$, is demonstrated. In the process we explain the practical computation of the frame $\mathbf{V}$ of Fig. 2, from the time sequences $a_i[n]$. SMV and MMV systems are solved using orthogonal matching pursuit [10, 11].

4.1. Selecting Sign Patterns

Calculating δ_K of $\mathbf{A} = \mathbf{SF}$ according to (14) is a combinatorial time-consuming procedure [8]. Instead, evaluating the stability can be implicitly performed as follows. Let $\mathbf{S} = \{\alpha_{ik}\}$ be the specific sign pattern under test and $\mathbf{F}$ as defined earlier. Prepare an extensive set of K-sparse vectors, by selecting the non-zeros locations uniformly at random and independently drawing the non-zero values from a normal distribution. If OMP (or any other preferred CS algorithm) succeeds to recover the K-sparse $\mathbf{x}$ from $\mathbf{y} = \mathbf{Ax}$ for most examples, then $\mathbf{A}$ can be assumed to have the RIP. Fig. 4 depicts results of such an experiment for 12 choices of $\mathbf{S}$ according to different strategies. The reported recovery rate is an average over 100 examples for every value of $1 \le K \le 10$. Constructing $\mathbf{S}$ by cyclic shifts of a single random row, is shown to be as stable as using a fully random $\mathbf{S}$. In contrast, trying to impose inter-row periodicity lead to a non-stable recovery, since $\delta_K = 0$ for $K \ge 2$ with this selection. The cyclic-shifts strategy can be used to reduce hardware complexity when implementing the m mixing functions [13]. Point out that this experiment differs from standard CS setups (*e.g.,* [6, 7, 10]) in which $\mathbf{S}$ is also randomly selected together with every $\mathbf{x}$. Here, the patterns under test remain fixed for the entire experiment.

4.2. Noisy Setting

To evaluate recovery from noisy input signals, an additive white Gaussian noise model is assumed at the system input, $x(t) + n(t)$. Our setup generates 100 multi band signals which are sampled with

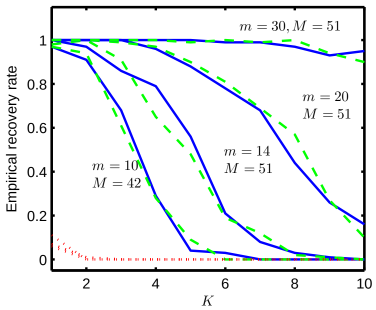

Fig. 4: Recovery performance for different selections of $\mathbf{S}$: fully random (solid), random $m \times 3$ signs matrix concatenated $M/3$ times (dotted), and cycle-shifts of a single random row (dashed).

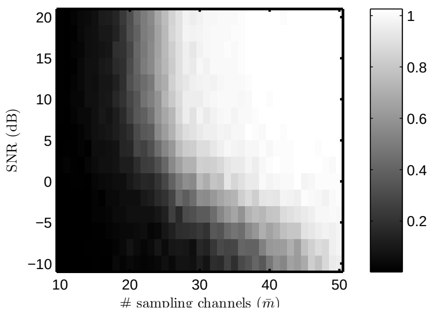

Fig. 5: Image intensity represents percentage of correct support set recovery $\hat{S} = S$, for reconstruction from different number of sampling sequences $\bar{m}$ and under several SNR levels.

$m = 51$ channels according to Fig. 3. The flow of Fig. 2 is used to recover an estimated support set $\hat{S}$ from only $\bar{m} \leq m$ sequences. The average recovery rate of $\hat{S} = S$, where S is the true support set, is reported in Fig. 5, as $\bar{m}$ varies from 6 to $\bar{m} = m$, and for different signal to noise ratios (SNR), defined by SNR(dB)=$10 \log(\|x\|/\|n\|)$ with L_2 norms.

To generate the 100 multi band signals, we choose $N = 3, B = 40$ MHz and $x(t) = \sum_{i=1}^{N} \sqrt{E_i B}\, \mathrm{sinc}(Bt) cos(2\pi f_i t)$, where $\mathrm{sinc}(x) = \sin(\pi x)/(\pi x)$ for $x \neq 0$ and $\mathrm{sinc}(x) = 1$ otherwise. The energy coefficients are fixed $E_i = \{1, 2, 3\}$, whereas for every signal the carriers f_i are chosen uniformly at random in $[-f_{\text{NYQ}}/2, f_{\text{NYQ}}/2]$ for $f_{\text{NYQ}} = 10$ GHz. A dense grid of 4000 equispaced points in the time interval $[-200/f_{\text{NYQ}}, 200/f_{\text{NYQ}}]$ is used to represent continuous signals on a computer. A white Gaussian noise is added and scaled to the desired SNR.

The parameters of the sampling stage are: $M = 51, T_s = T_p = M/f_{\text{NYQ}}$. The values $\alpha_{ik} = \pm 1$ are drawn randomly with equal probability and remain fixed for the entire experiment. At the ith channel, the dense samples of $x(t) + n(t)$ are multiplied by $p_i(t)$ and passed to a 50-tap low-pass filter, designed by the MATLAB command h=fir1(50,1/M). The output is decimated to produce the low-rate sequences $a_i[n]$.

Note that constructing the frame $\mathbf{V}$ of Fig. 2 is carried out by first computing the m-squared values $\mathbf{Q}_{ik} = \sum_n a_i[n] a_k[n]$, and then using the eigenvalue decomposition $\mathbf{Q} = \mathbf{V}\mathbf{V}^H$ while discarding eigenvectors of the noise space [3].

5. CONCLUSIONS

We developed an efficient sampling stage for analog multi band signals. In the proposed system, analog mixers and standard ADCs replace impractical non uniform sampling of multi coset strategy. Analog mixers for wideband applications is an existing RF technology, though selecting the exact devices requires an expertise in analog design.

The proposed system has a set of parameters, which determines the signal, if selected according to the conditions we derived. Analyzing our system in the frequency domain lead to an IMV system, which allows to use existing reconstruction stages with only minor modifications. In addition, based on the IMV system and recent works in the CS literature, we deduce the rate requirements for stable blind recovery, which in general is higher than the rate required to determine the signal from its samples.

A preliminary computer evaluation of our system shows a promise for stable blind recovery from sub-Nyquist sampling rate, although further work is required to quantify the optimal working point in the trade-off between sampling rate, blindness, and practical implementation.

6. REFERENCES

[1] Y.-P. Lin and P. P. Vaidyanathan, “Periodically nonuniform sampling of bandpass signals,” *IEEE Trans. Circuits Syst. II*, vol. 45, no. 3, pp. 340–351, Mar. 1998.

[2] R. Venkataramani and Y. Bresler, “Perfect reconstruction formulas and bounds on aliasing error in sub-nyquist nonuniform sampling of multiband signals,” *IEEE Trans. Inf. Theory*, vol. 46, no. 6, pp. 2173–2183, Sep. 2000.

[3] M. Mishali and Y. C. Eldar, “Blind multi-band signal reconstruction: Compressed sensing for analog signals,” *CCIT Report no. 639, EE Dept., Technion - Israel Institute of Technology; submitted to IEEE Trans. Signal Process.*, Sep. 2007.

[4] M. Fleyer, A. Rosenthal, A. Linden, and M. Horowitz, “Multirate synchronous sampling of sparse multiband signals,” *Arxiv preprint arXiv:0806.0579*, 2008.

[5] J. N. Laska, S. Kirolos, M. F. Duarte, T. S. Ragheb, R. G. Baraniuk, and Y. Massoud, “Theory and implementation of an analog-to-information converter using random demodulation,” in *Proc. of. ISCAS 2007*, 2007, pp. 1959–1962.

[6] M. Mishali and Y. C. Eldar, “Reduce and boost: Recovering arbitrary sets of jointly sparse vectors,” *IEEE Trans. Signal Process.*, vol. 56, no. 10, pp. 4692–4702, Oct. 2008.

[7] J. Chen and X. Huo, “Theoretical results on sparse representations of multiple-measurement vectors,” *IEEE Trans. Signal Process.*, vol. 54, no. 12, pp. 4634–4643, Dec. 2006.

[8] E. J. Candès, J. Romberg, and T. Tao, “Robust uncertainty principles: Exact signal reconstruction from highly incomplete frequency information,” *IEEE Trans. Inf. Theory*, vol. 52, no. 2, pp. 489–509, Feb. 2006.

[9] D. L. Donoho, “Compressed sensing,” *IEEE Trans. Inf. Theory*, vol. 52, no. 4, pp. 1289–1306, April 2006.

[10] S. F. Cotter, B. D. Rao, K. Engan, and K. Kreutz-Delgado, “Sparse solutions to linear inverse problems with multiple measurement vectors,” *IEEE Trans. Signal Process.*, vol. 53, no. 7, pp. 2477–2488, July 2005.

[11] J. A. Tropp, A. C. Gilbert, and M. J. Strauss, “Algorithms for simultaneous sparse approximation. Part I: Greedy pursuit,” *Signal Process.*, vol. 86, pp. 572–588, Apr. 2006.

[12] J. A. Tropp, “Algorithms for simultaneous sparse approximation. Part II: Convex relaxation,” *Signal Process.*, vol. 86, pp. 589–602, Apr. 2006.

[13] M. Mishali, Y. C. Eldar, and J. A. Tropp, “Efficient sampling and stable reconstruction of wide band sparse analog signals,” *CCIT Report, EE Dept., Technion - Israel Institute of Technology*, Oct. 2008.

[14] R. Baraniuk, M. Davenport, R. DeVore, and M. Wakin, “A simple proof of the restricted isometry property for random matrices,” *Const. Approx.*, 2007.

[15] T. Blumensath and M. E. Davies, “Sampling theorems for signals from the union of linear subspaces,” *preprint*, 2007.